UC San Diego
UC San Diego Previously Published Works

## Title
Emissive Synthetic Cofactors: An Isomorphic, Isofunctional, and Responsive NAD+ Analogue

**Permalink**
https://escholarship.org/uc/item/8tf240mx

**Journal**
Journal of the American Chemical Society, 139(44)

**ISSN**
0002-7863

**Authors**
Rovira, Alexander R
Fin, Andrea
Tor, Yitzhak

**Publication Date**
2017-11-08

**DOI**
10.1021/jacs.7b05852

Peer reviewed

eScholarship.org Powered by the California Digital Library
University of California

HHS Public Access
Author manuscript
*J Am Chem Soc*. Author manuscript; available in PMC 2018 November 08.

Published in final edited form as:
*J Am Chem Soc*. 2017 November 08; 139(44): 15556–15559. doi:10.1021/jacs.7b05852.

# Emissive Synthetic Cofactors: An Isomorphic, Isofunctional, and Responsive $NAD^+$ Analogue

**Alexander R. Rovira**, **Andrea Fin**, and **Yitzhak Tor***
Department of Chemistry and Biochemistry, University of California, San Diego, La Jolla, California 92093-0358, United States

## Abstract

The synthesis, photophysics, and biochemical utility of a fluorescent $NAD^+$ analogue based on an isothiazolo[4,3-*d*]pyrimidine core (**N$^{tz}$AD$^+$**) are described. Enzymatic reactions, photophysically monitored in real time, show **N$^{tz}$AD$^+$** and **N$^{tz}$ADH** to be substrates for yeast alcohol dehydrogenase and lactate dehydrogenase, respectively, with reaction rates comparable to that of the native cofactors. A drop in fluorescence is seen as **N$^{tz}$AD$^+$** is converted to **N$^{tz}$ADH**, reflecting a complementary photo-physical behavior to that of the native $NAD^+$/NADH. **N$^{tz}$AD$^+$** and **N$^{tz}$ADH** serve as substrates for NADase, which selectively cleaves the nicotinamide's glycosidic bond yielding **$^{tz}$ADP-ribose. N$^{tz}$AD$^+$** also serves as a substrate for ribosyl transferases, including human adenosine ribosyl transferase 5 (ART5) and Cholera toxin subunit A (CTA), which hydrolyze the nicotinamide and transfer **$^{tz}$ADP-ribose** to an arginine analogue, respectively. These reactions can be monitored by fluorescence spectroscopy, in stark contrast to the corresponding processes with the nonemissive $NAD^+$.

---

Modified oligonucleotides represent a fraction of the innovative ways for exploiting fluorescent nucleoside analogues.[1] The vast biochemistry of nucleosides and nucleotides as coenzymes and secondary messengers offers unique opportunities for their emissive surrogates as biophysical and mechanistic tools. Pioneered by giants such as Leonard and Shugar, most early studies were done with perturbing emissive nucleoside analogues (e.g., 1,$N^6$-ethenoadenosine) or poorly emissive ones (e.g., 8-azapurines).[2,3] A key principle for the universal implementation of such probes is to minimize structural and functional perturbations, which are inevitable consequences of replacing any native residue with a synthetic analogue. We define nucleosides that fulfill such critical constraints as being isomorphic and isofunctional, respectively. To serve as effective emissive probes, at least one

---

*Corresponding Author: ytor@ucsd.edu.
**ORCID**
Andrea Fin: 0000-0002-7567-4646
Yitzhak Tor: 0000-0003-3726-7799

**Notes**
The authors declare the following competing financial interest(s): Yitzhak Tor provides consulting services to TriLink Biotechnologies. The terms of the arrangements have been reviewed and approved by the University of California, San Diego in accordance with its conflict of interest policies.

Supporting Information
The Supporting Information is available free of charge on the ACS Publications website at DOI: 10.1021/jacs.7b05852.
Synthetic and analytical details, photophysical data, enzymatic protocols, and HPLC traces (PDF)

Author Manuscript
Author Manuscript
Author Manuscript
Author Manuscript

Author Manuscript Author Manuscript Author Manuscript Author Manuscript

of the analogue's photophysical characteristics must respond to structural and environmental changes. We describe such an attribute as responsiveness.[4]

$NAD^+$ and NADH (Figure 1), the corresponding reduced form, are key determinants of the cellular redox state.[5] In addition to its metabolic roles and extracellular signaling functions,[6] $NAD^+$ is also a substrate for several key enzymes, including poly-ADP-ribose polymerases (PARP), mono-ADP-ribose transferases (ART), sirtuins, cyclases, and DNA ligases.[7–10] Its involvement in metabolic and regulatory processes makes $NAD^+$ a key cofactor and its emissive analogues have been explored for decades.[11] One $NAD^+$ analogue that has been widely employed is 1,*N*[6]-etheno $NAD^+$ ($\varepsilon NAD^+$), originally introduced by Leonard and coworkers.[12] Enzymatic cleavage at the nicotinamide moiety (forming the corresponding nicotinamide and *ε*–adenosine diphosphate riboside) is required to induce a large change in $\varepsilon NAD^+$'s emission quantum yield.[13–15] Other nonisomorphic fluorescent $NAD^+$ analogues have been developed for similar applications,[11b] and a clickable version was recently reported.[11c,16] Intriguingly, while the reduced native cofactor, NADH, is emissive ($\lambda_{em}$ 460 nm, $\Phi$ = 0.02),[17] the native $NAD^+$ is not. We thus sought to develop an isomorphic and isofunctional redox couple with orthogonal photophysical behavior to the native substrate (Figure 1). Such a synthetic cofactor could expand the processes that can be visualized in real-time by fluorescence spectroscopy.[18]

Our lab has developed a family of emissive isomorphic and isofunctional ribonucleosides based on an isothiazolo[3,4-*d*] pyrimidine core.[19] Considering the red-shifted absorption band and emissive nature of NADH relative to $NAD^+$,[17,20] we hypothesized that by replacing adenosine with **$^{tz}$A** (Figure 1, Scheme 1), our fluorescent adenosine analogue, an emissive $NAD^+$ analogue with distinct photophysical features and the potential to enhance the spectroscopic monitoring of $NAD^+$-dependent processes will be obtained.

Herein we report the synthesis, photophysics, and enzymatic interconversions of **N$^{tz}$AD$^+$**, an $NAD^+$ analogue based on our isomorphic isothiazolo heterocyclic system that is emissive and isofunctional. While the **N$^{tz}$AD$^+$/N$^{tz}$ADH** couple is complementary in its photophysical behavior to that of the native cofactors $NAD^+$/NADH, the emissive **N$^{tz}$AD$^+$** facilitates the fluorescence-based monitoring of ADP-ribosylation reactions, which are "fluorescently-silent" with the native cofactor.

To prepare **N$^{tz}$AD$^+$**, the previously synthesized **$^{tz}$A**[19] was treated with $POCl_3$ and trimethyl phosphate to give **$^{tz}$AMP** (Scheme 1), which was coupled to activated *β*-nicotinamide mononucleotide following published protocols.[11c,21] The spectroscopic properties of **N$^{tz}$AD$^+$** closely resemble that of **$^{tz}$A**, the core nucleoside. The absorption and emission maxima are found to be 336 and 411 nm, respectively, with a fluorescence quantum yield of 3.8 ± 0.4% (Table 1).

The biocompatibility and photophysical responsiveness of **N$^{tz}$AD$^+$** were initially tested with *Saccharomyces cerviseae* alcohol dehydrogenase (ADH). This dehydrogenase catalyzes the reversible oxidation of ethanol to acetaldehyde, using $NAD^+$ as a cofactor (Figure 2a). When subjecting **N$^{tz}$AD$^+$** to ADH and ethanol in buffer (pH 7.6), the conversion to the corresponding **N$^{tz}$ADH** was effectively monitored via a large decrease in its visible fluorescence intensity ($\lambda_{ex}$ 330 nm, $\lambda_{em}$ 410 nm) and increase in absorbance at 330 nm (Figure 2b).[21]

Subjecting $NAD^+$ to the same enzymatic reaction with ADH under the same conditions yielded a comparable rate with $t_{1/2}$ = 23 ± 3 and 21 ± 1 s for $NAD^+$ and $\mathbf{N^{tz}AD^+}$, respectively (Figure S4 and Table S2). The reaction was then reversed by adding excess acetaldehyde after the initial dehydrogenation was complete. The fluorescence signal was restored within seconds (Figure S5). Similarly, HPLC reaction monitoring showed near-full conversion of $\mathbf{N^{tz}AD^+}$ to $\mathbf{N^{tz}ADH}$ after 5 min followed by instantaneous regeneration of the former following the addition of acetaldehyde (Figure 2c).[21]

To further challenge our emissive $NAD^+$ analogue and assess its biochemical compatibility, it was tested with lactate dehydrogenase (LDH), a metabolic enzyme catalyzing the interconversion of pyruvate to lactate and concurrently NADH to $NAD^+$.[22] After consumption of $\mathbf{N^{tz}AD^+}$ with ADH and ethanol, the reaction is treated with pyruvic acid followed by LDH. The reformation of $\mathbf{N^{tz}AD^+}$ from $\mathbf{N^{tz}ADH}$ shows nearly full restoration of fluorescence intensity (Figure 2d, red/orange). This behavior was complementary to that of $NAD^+$, essentially mirroring its time course, which shows enhanced emission at 465 nm, arising from the formation of NADH, followed by a subsequent decrease in emission after the addition of LDH (Figure 2d, gray).

To shed light on the photophysical behavior of $\mathbf{N^{tz}AD^+}$ and $\mathbf{N^{tz}ADH}$, their response upon enzymatic cleavage of the nicotinamide moiety with porcine brain NADase was evaluated (Figure 3). NADase specifically cleaves $NAD^+$ at the nicotinamide-ribose linkage, yielding nicotinamide and ADP-ribose (ADPR).[12,23] Treating $\mathbf{N^{tz}ADH}$ (generated from $\mathbf{N^{tz}AD^+}$ with ADH and ethanol) with NADase yielded a net 30% emission enhancement above the initial level before treatment with ADH (Figure 3b,c). Upon treatment of $\mathbf{N^{tz}AD^+}$ with NADase, a 40% increase in emission was observed (Figure 3c, inset). We hypothesize that the diminished emission observed upon reducing $\mathbf{N^{tz}AD^+}$ to $\mathbf{N^{tz}ADH}$ could arise from static quenching or a filtering effect by the reduced nicotinamide moiety, noting that NADH absorbs at nearly the same wavelength as $\mathbf{^{tz}A}$ (Table 1). The observed emission enhancement upon treatment with NADase and subsequent conversion to $\mathbf{^{tz}ADP\text{-}ribose}$ (Figure 3) suggests, however, that the photophysics of these molecules is influenced by a myriad of intramolecular ground and excited state interactions between the nicotinamide and $\mathbf{^{tz}A}$ moieties. These may include a combination of filter effects, photoinduced electron transfer (PET), and additional quenching pathways arising from proximity-driven interactions between the nicotinamide and isothiazolopyrimidine core, as reported for $NAD^+$ and related analogues.[13a,17,20,24]

Finally, to illustrate the unique features of the emissive $\mathbf{N^{tz}AD^+}$ compared to the nonemissive $NAD^+$ and take advantage of the photophysical changes induced upon cleavage of the nicotinamide moiety, we have expanded the enzymatic processes monitored to ADP ribosyl transfer reactions.[25] While several enzyme classes exploit $NAD^+$ through cleavage of the nicotinamide (e.g., PARPs, sirtuins), we employed arginine-specific mono-ADP-ribose transferases (ARTs), as they facilitate clearer detection of reactivity and biocompatibility. Two commercially available proteins with reported mono-ADP-ribosylation activity were



Author Manuscript Author Manuscript Author Manuscript Author Manuscript

Author Manuscript Author Manuscript Author Manuscript Author Manuscript

used: human ART5, a transferase originally cloned from Yac-1 lymphoma cells in mice,[26] and Cholera toxin subunit A (CTA),[27] derived from Cholera toxin, a protein from the $AB_5$ toxin family. While arginine-specific ARTs operate in diverse biological systems and are regulated in complex manners,[25,28] we chose ART5 as it has been identified as a major producer of arginine-specific ADP-ribose modification[29] and CTA, as it has been well-studied as an arginine-specific ADPR transferase.[30]

Upon treatment with ART5 and agmatine (a commonly used Arg surrogate in ART assays),[29] both $NAD^+$ and **$N^{tz}AD^+$** were found to primarily undergo hydrolysis, under a variety of conditions, forming ADP-ribose and **$^{tz}$ADP-ribose**, respectively (Figure 4). This process, which has been documented for $NAD^+$,[26a,29] was found to occur at the same rate (Figure 4b), as detected via emission (for $N^{tz}AD^+$) and HPLC (for both $NAD^+$ and $N^{tz}AD^+$).[31] Upon treatment with CTA and agmatine, both $NAD^+$ and **$N^{tz}AD^+$** were found to produce primarily **ADPR-agmatine** and **$^{tz}$ADPR-agmatine**, respectively, as monitored via emission (for **$N^{tz}AD^+$**) and HPLC (for both $NAD^+$ and **$N^{tz}AD^+$**) (Figure 4c). These reactions show complete consumption of the corresponding substrates within 90 min, and formation of roughly 10% of ADPR or **$^{tz}$ADPR** as minor hydrolysis products. **$N^{tz}AD^+$** seemed to react slightly slower than the native cofactor with CTA. Importantly, however, **$^{tz}$ADPR-agmatine** was found to have near identical photo-physical properties as **$^{tz}$A**, thus facilitating the fluorescence-based monitoring of the enzyme-mediated ADP-ribosylation.[32]

While the reactions of **$N^{tz}AD^+$** with alcohol and lactate dehydrogenase exemplify the isofunctionality of our emissive cofactor within the context of biochemically relevant redox reactions, its reactivity with mono ADP-ribose transferases reinforces this notion. In particular, the suitability of **$N^{tz}AD^+$** as a substrate for ADP ribosyl transferases, key enzymes responsible for diverse post-transcriptional modifications of cellular regulatory significance,[25] illustrated with CTA-mediated **$^{tz}$ADP**-ribosylation of agmatine, showcases the formation of a new glycoside linkage to an amino acid derivative. Above all and in stark contrast to the nonemissive native $NAD^+$, such processes yield fluorescent ribosylated products and can be kinetically monitored by enhanced fluorescence signals, due to the displacement of the quenching nicotinamide moiety.

In summary, the isothiazolo[4,3-*d*]pyrimidine-based $NAD^+$ analogue displays isofunctionality and complementary photo-physical behavior when compared to its native counterpart, with the oxidized form (**$N^{tz}AD^+$**) being much more emissive than the reduced one (**$N^{tz}$ADH**). To our knowledge, no fluorescent $NAD^+$ analogues with photophysical behavior complementary to the native $NAD^+$ and NADH couple have been previously reported. Furthermore, **$N^{tz}AD^+$** serves as faithful substrate for ADP-ribose transferases. Unlike the nonemissive $NAD^+$, **$N^{tz}AD^+$** facilitates the kinetic monitoring of enzymatic hydrolysis and transferase activities by fluorescence spectroscopy and yields visibly fluorescent products. **$N^{tz}AD^+$** has thus been subjected to five enzymes, which share common mechanistic pathways with most other $NAD^+$-utilizing reactions, where the nicotinamide moiety serves as either a redox unit or as a leaving group. A synthetic cofactor such as **$N^{tz}AD^+$**, with unprecedented photophysical responses and biocompatibility, could therefore

Author Manuscript Author Manuscript Author Manuscript Author Manuscript

enhance and expand the real-time visualization of cofactor-dependent processes by fluorescence spectroscopy.

## Supplementary Material

Refer to Web version on PubMed Central for supplementary material.

## Acknowledgments

We thank the National Institutes of Health for generous support (GM 069773) and UCSD's Chemistry and Biochemistry MS Facility.

## References


1. Sinkeldam RW, Greco NJ, Tor Y. Chem Rev. 2010; 110:2579–2619. [PubMed: 20205430]
2. Leonard NJ, Barrio JR. Crit Rev Biochem. 1984; 15:125–199. [PubMed: 6365449]
3. Wierzchowski J, Antosiewicz JM, Shugar D. Mol BioSyst. 2014; 10:2756–2774. [PubMed: 25124808]
4. Sinkeldam RW, Tor Y. Org Biomol Chem. 2007; 5:2523–2528. [PubMed: 18019524]
5. (a) Everse, J., Anderson, B., You, K. The Pyridine nucleotide coenzymes. Academic Press; New York: 1982. (b) Ying WH. Antioxid Redox Signaling. 2008; 10:179–206.(c) Collins Y, Chouchani ET, James AM, Menger KE, Cocheme HM, Murphy MP. J Cell Sci. 2012; 125:801–806. [PubMed: 22448036]
6. Garten A, Schuster S, Penke M, Gorski T, de Giorgis T, Kiess W. Nat Rev Endocrinol. 2015; 11:535–546. [PubMed: 26215259]
7. (a) Chambon P, Mandel P, Weill JD. Biochem Biophys Res Commun. 1963; 11:39–43. [PubMed: 14019961] (b) Hayaishi O, Veda K. Annu Rev Biochem. 1977; 46:95–116. [PubMed: 197884] (c) Cervantes-Laurean D, Minter DE, Jacobson EL, Jacobson MK. Biochemistry. 1993; 32:1528–1534. [PubMed: 8431431] (d) Hassa PO, Haenni SS, Elser M, Hottiger MO. Microbiol Mol Biol Rev. 2006; 70:789–829. [PubMed: 16959969]
8. (a) Boulikas T. Anticancer Res. 1991; 11:489–527. [PubMed: 1905900] (b) Hottiger MO. Annu Rev Biochem. 2015; 84:227–263. [PubMed: 25747399]
9. Bonkowski MS, Sinclair DA. Nat Rev Mol Cell Biol. 2016; 17:679–690. [PubMed: 27552971]
10. Moss J, Stanley SJ. J Biol Chem. 1981; 256:7830–7833. [PubMed: 6267027]
11. (a) Pankiewicz KW, Watanabe KA, Lesiak-Watanabe K, Goldstein BM, Jayaram HN. Curr Med Chem. 2002; 9:733–741. [PubMed: 11966436] (b) Pergolizzi G, Butt JN, Bowater RP, Wagner GK. Chem Commun. 2011; 47:12655–12657.(c) Wang Y, Rosner D, Grzywa M, Marx A. Angew Chem, Int Ed. 2014; 53:8159–8162.
12. Barrio JR, Secrist JA, Leonard NJ. Proc Natl Acad Sci U S A. 1972; 69:2039–2042. [PubMed: 4340748]
13. (a) Gruber BA, Leonard NJ. Proc Natl Acad Sci U S A. 1975; 72:3966–3969. [PubMed: 172889] (b) Luisi PL, Baici A, Bonner FJ, Aboderin AA. Biochemistry. 1975; 14:362–368. [PubMed: 164204]
14. Lee CY, Everse J. Arch Biochem Biophys. 1973; 157:83–90. [PubMed: 4352059]
15. To our knowledge, the enzymatic conversion of $\varepsilon NAD^+$ to $\varepsilon$NADH has not been photophysically studied. The cofactors have shown photophysical differences when bound to GDH: Dieter H, Koberstein R, Sund H. FEBS Lett. 1974; 47:90–93. [PubMed: 4372090]
16. Willner has electrochemically studied surface-bound cofactors; See: Bardea A, Katz E, Bückmann AF, Willner I. J Am Chem Soc. 1997; 119:9114–9119.Katz E, Willner I. Angew Chem, Int Ed. 2004; 43:6042–6108.
17. Scott TG, Spencer RD, Leonard NJ, Weber G. J Am Chem Soc. 1970; 92:687–695.

Author Manuscript Author Manuscript Author Manuscript Author Manuscript

18. (a) Vranken C, Fin A, Tufar P, Hofkens J, Burkart MD, Tor Y. Org Biomol Chem. 2016; 14:6189–6192. [PubMed: 27270873] (b) Deen J, Vranken C, Leen V, Neely RK, Janssen KPF, Hofkens J. Angew Chem, Int Ed. 2017; 56:5182–5200.
19. (a) Rovira AR, Fin A, Tor Y. J Am Chem Soc. 2015; 137:14602–14605. [PubMed: 26523462] (b) Rovira AR, Fin A, Tor Y. Chem Sci. 2017; 8:2983–2993. [PubMed: 28451365]
20. Hull RV, Conger PS III, Hoobler RJ. Biophys Chem. 2001; 90:9–16. [PubMed: 11321678]
21. See Supporting Information for experimental details.
22. (a) Månsson MO, Larsson PO, Mosbach K. FEBS Lett. 1979; 98:309–313. [PubMed: 217734] (b) Chenault HK, Whitesides GM. Bioorg Chem. 1989; 17:400–409.(c) Faber, K. Biotransformations in organic chemistry. Springer-Verlag; Berlin: 1992.
23. Kaplan NO, Colowick SP, Nason A. J Biol Chem. 1951; 191:473–483. [PubMed: 14861193]
24. Tanaka M, Ohkubo K, Fukuzumi S. J Phys Chem A. 2006; 110:11214–11218. [PubMed: 16986858]
25. Koch-Nolte, F., editor. Endogenous ADP-Ribosylation. Springer International Publishing; Cham, Switzerland: 2015.
26. (a) Weng BY, Thompson WC, Kim HJ, Levine RL, Moss J. J Biol Chem. 1999; 274:31797–31803. [PubMed: 10542202] (b) Okazaki IJ, Moss J. Annu Rev Nutr. 1999; 19:485–509. [PubMed: 10448534]
27. Vanden Broeck D, Horvath C, De Wolf MJ. Int J Biochem Cell Biol. 2007; 39:1771–5. [PubMed: 17716938]
28. (a) Moss J, Stanley SJ, Osborne JC Jr. J Biol Chem. 1981; 256:11452–6. [PubMed: 6271751] (b) Hottiger MO, Hassa PO, Luscher B, Schuler H, Koch-Nolte F. Trends Biochem Sci. 2010; 35:208–219. [PubMed: 20106667]
29. Glowacki G, Braren R, Firner K, Nissen M, Kuhl M, Reche P, Bazan F, Cetkovic-Cvrlje M, Leiter E, Haag F, Koch-Nolte F. Protein Sci. 2002; 11:1657–1670. [PubMed: 12070318]
30. (a) Moss J, Vaughan M. J Biol Chem. 1977; 252:2455–2457. [PubMed: 139409] (b) Tsai SC, Noda M, Adamik R, Moss J, Vaughan M. Proc Natl Acad Sci U S A. 1987; 84:5139–42. [PubMed: 3110784]
31. High levels of glycohydrolase activity versus transferase activity have been reported for ART5. See reference 29.
32. $^{\mathbf{tz}}$**ADP-ribose** and $^{\mathbf{tz}}$**ADPR-agmatine** have the same photo-physical properties as $^{\mathbf{tz}}$**A**, the parent nucleoside. See SI and Figures S9 and S15.

Author Manuscript Author Manuscript Author Manuscript Author Manuscript

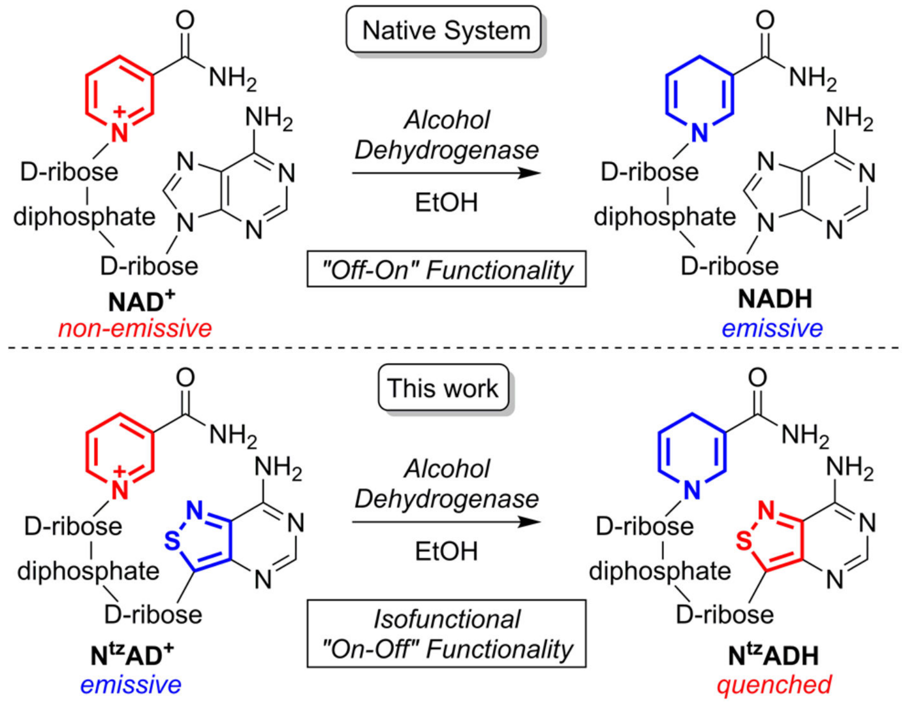


**Figure 1.**

Comparing the photophysical behavior of native $NAD^+$ and $\mathbf{N^{tz}AD^+}$ in reactions involving alcohol dehydrogenase.

Author Manuscript

Author Manuscript

Author Manuscript

Author Manuscript



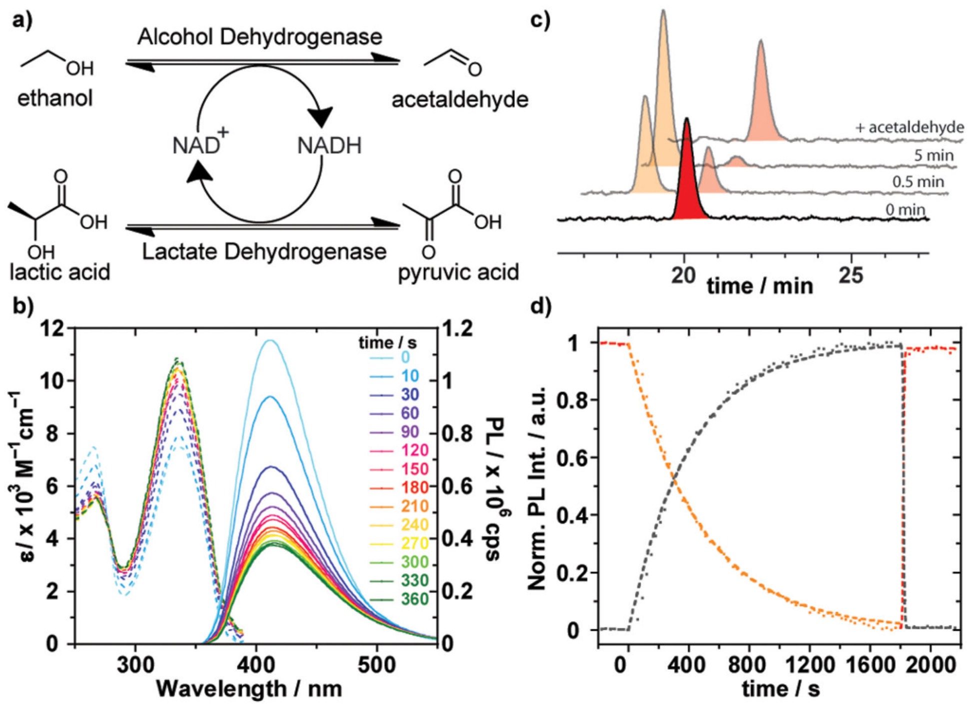


**Figure 2.**

(a) Enzymatic cycle for $NAD^+$ consumption and regeneration with ADH and LDH. (b) ADH-mediated oxidation of ethanol to acetaldehyde using **$N^{tz}AD^+$** followed by UV and fluorescence spectroscopies ($\lambda_{ex}$ = 330 nm). (c) As in b, showing **$N^{tz}AD^+$** (red) to **$N^{tz}ADH$** (orange) conversion, followed by HPLC (monitored at 330 nm). (d) ADH-mediated oxidation of ethanol to acetaldehyde followed by LDH-mediated reduction of pyruvic acid to lactic acid with **$N^{tz}AD^+$** (red/orange) and $NAD^+$ (gray) followed by real-time emission at 410 nm ($\lambda_{ex}$ = 330 nm) and 465 nm ($\lambda_{ex}$ = 335 nm), respectively. Dashed lines represent weighted curve fits.[21]

Author Manuscript Author Manuscript Author Manuscript Author Manuscript

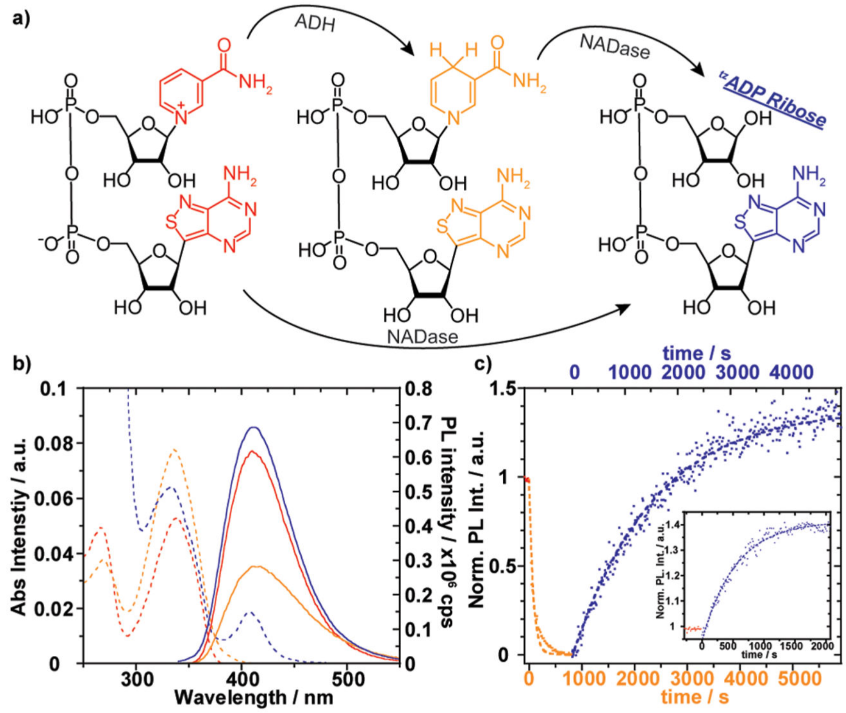


**Figure 3.**

(a) Enzymatic cycle for **N$^{tz}$AD$^{+}$** consumption by ADH and NADase. (b) UV–vis and emission ($\lambda_{ex}$ = 330 nm) spectra of **N$^{tz}$AD$^{+}$** at time 0 (red), after oxidizing ethanol to acetaldehyde with ADH (orange) and subsequent treatment with NADase (blue). (c) Real-time emission intensity at 410 nm ($\lambda_{ex}$ = 330 nm) of the enzymatic oxidation of ethanol to acetaldehyde by ADH with **N$^{tz}$AD$^{+}$** (orange, bottom time scale) followed by cleavage with NADase (blue, top time scale). Inset: Cleavage of **N$^{tz}$AD$^{+}$** with NADase (blue) followed by real-time emission at 410 nm ($\lambda_{ex}$ = 330 nm).

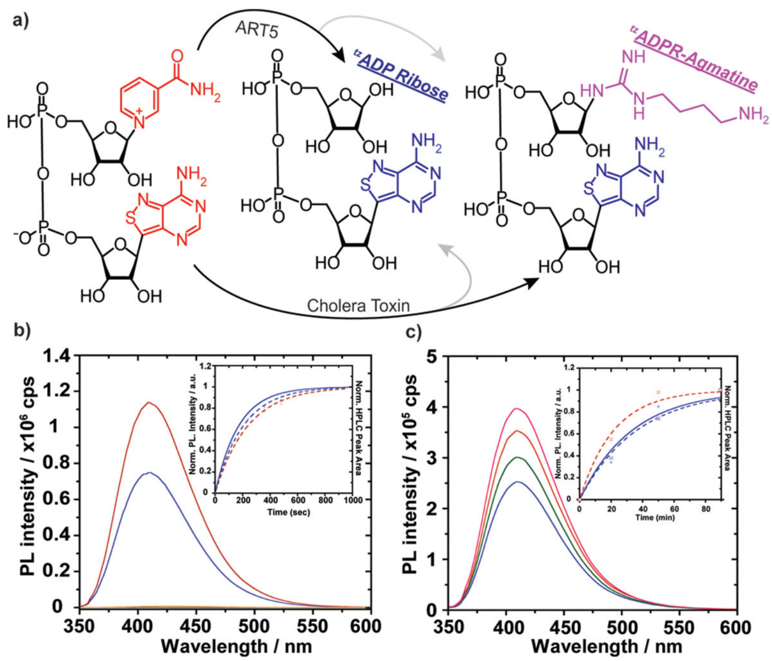


**Figure 4.**

(a) Treatment of **N$^{tz}$AD$^+$** with ART5 and CTA to yield ADPR and ADPR-agmatine, respectively. (b) Steady state emission spectra following treatment of **N$^{tz}$AD$^+$** with ART5[21] at 0 (blue) and 18 min (red), as well as NAD$^+$ at 0 (green) and 18 min (orange), $\lambda_{ex}$ = 335 nm. Inset: Fluorescence based kinetics of aforementioned reaction ($\lambda_{em}$ = 410 nm, $\lambda_{ex}$ = 335 nm, blue solid), and normalized HPLC-monitored product formation from reactions with **N$^{tz}$AD$^+$** (blue, dashed) and native NAD (red, dashed). (c) Steady state emission spectra ($\lambda_{ex}$ = 335 nm) following treatment of **N$^{tz}$AD$^+$** with CTA;[21] reaction sampled at 0 (blue), 20 (green), 50 (orange), and 90 min (pink). Inset: Reactions with CTA following normalized emission intensity at 410 nm ($\lambda_{ex}$ = 335 nm, blue, solid), normalized HPLC-monitored product formation from reactions with **N$^{tz}$AD$^+$** (blue, dashed) and native NAD$^+$ (red, dashed).[21]



Author Manuscript Author Manuscript Author Manuscript Author Manuscript

Author Manuscript Author Manuscript Author Manuscript Author Manuscript

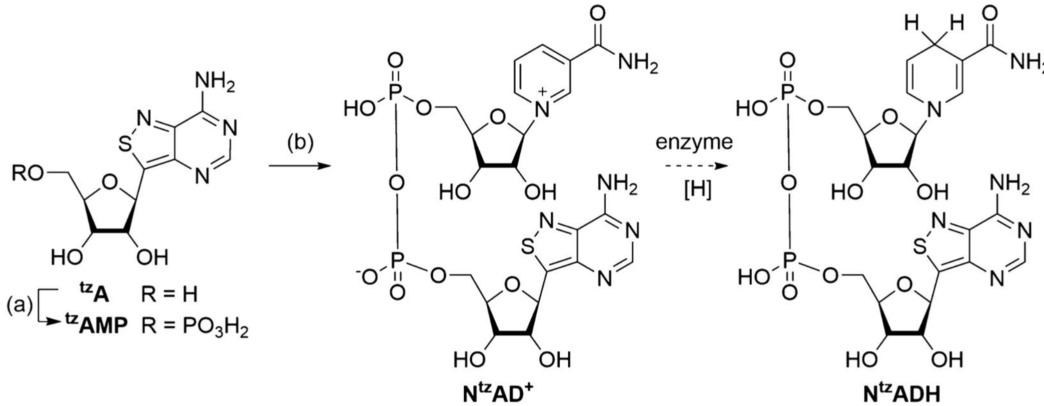


**Scheme 1. Synthesis of N$^{tz}$AD**

[a]Reagents and conditions: (a) $POCl_3$, proton sponge, trimethyl phosphate, 4 °C, 2 h, 50%. (b) i. *β*-Nicotinamide mononucleotide, CDI, $Et_3N$, DMF, rt, 6 h; ii. **$^{tz}$AMP**, DMF, rt, 4 days, 20%.[21]

Author Manuscript

Author Manuscript

Author Manuscript

Author Manuscript

**Table 1**

Photophysical Properties

| | $\lambda_{abs}$ ($\varepsilon$)[a] | $\lambda_{em}$ ($\Phi$)[a] | Stokes shift[a] |
|---|---|---|---|
| **$^{tz}$A**[b] | 338 (7.79) | 410 (0.05) | 5.23 |
| **N$^{tz}$AD$^{+}$**[c] | 336 (6.9) | 411 (0.038) | 5.41 |
| **N$^{tz}$AD$^{+}$**[d] | 338 (7.2) | 411 (0.044) | 5.23 |
| **N$^{tz}$ADH**[d,e] | 336 (10.7) | 412 (0.015) | 5.49 |
| NAD$^{+}$[b] | 259 (16.9) | | |
| NADH[b] | 339 (6.22) | 460 (0.02) | 7.76 |

[a] $\lambda_{abs}$, $\varepsilon$, $\lambda_{em}$ and Stokes shift are in nm, $10^3$ $M^{-1}$ $cm^{-1}$, nm, and $10^3$ $cm^{-1}$, respectively. All values reflect the average of at least three independent measurements. See Table S1 for experimental errors.

[b] See references 17 and 19.

[c] Measured in Milli-Q water.

[d] Measured in Tris buffer pH 7.6.

[e] Measured at ADH reaction end, assuming complete consumption, Tris buffer pH 7.6.